Published in final edited form as:
J Struct Biol. 2011 April ; 174(1): 100–106. doi:10.1016/j.jsb.2010.11.013.

Possible role of DMP1 in dentin mineralization

Elia Beniash[*], **Atul S. Deshpande**, **Ping An Fang**, **Nicholas S. Lieb**, **Xiaoyuan Zhang**, and **Charles S. Sfeir**[*]
Department of Oral Biology, Center for Craniofacial Regeneration, University of Pittsburgh School of Dental Medicine, Pittsburgh, PA

Abstract

Dentin Matrix Protein 1 (DMP1), the essential noncollagenous proteins in dentin and bone, is believed to play an important role in the mineralization of these tissues, although the mechanisms of its action are not fully understood. To gain insight into DMP1 functions in dentin mineralization we have performed immunomaping of DMP1 in fully mineralized rat incisors and *in vitro* calcium phosphate mineralization experiments in the presence of DMP1. DMP1 immunofluorescene was localized in peritubular dentin (PTD) and along the dentin-enamel boundary. In vitro phosphorylated DMP1 induced the formation of parallel arrays of crystallites with their *c*-axes co-aligned. Such crystalline arrangement is a hallmark of mineralized collagen fibrils of bone and dentin. Interestingly, in DMP1-rich PTD, which lacks collagen fibrils, the crystals are organized in a similar manner. Based on our findings we hypothesize, that *in vivo* DMP1 controls the mineral organization outside of the collagen fibrils and plays a major role in the mineralization of PTD.

Keywords

SIBLING PROTEINS; CARBONATED APATITE; HYDROXYAPATITE; SELF ASSEMBLY; DEJ

Introduction

DMP1, also called AG1 in the early literature, is an acidic noncollagenous phosphoprotein originally found in teeth (George *et al.*, 1993), but later also detected in bones (Hirst *et al.*, 1997; MacDougall *et al.*, 1998), where it is primarily expressed by osteocytes (Toyosawa *et al.*, 2001). DMP1 is a multifunctional protein involved in the biomineralization of bones and dentin (Ling *et al.*, 2005; Lu *et al.*, 2007; Qin *et al.*, 2004), phosphate homeostasis (Feng *et al.*, 2006), and differentiation of odonto- and osteoblasts (Almushayt *et al.*, 2006; Narayanan *et al.*, 2001). Mutations in this gene cause autosomal recessive hypophosphatemic rickets syndrome, manifested by rickets and osteomalacia with isolated renal phosphate-wasting (Feng *et al.*, 2006; Lorenz-Depiereux *et al.*, 2006). DMP1 belongs to the SIBLING (Small

[*]Corresponding authors: Elia Beniash, PhD, Associate Professor, Oral Biology, University of Pittsburgh School of Dental Medicine, Center for Craniofacial Regeneration, McGowan Institute for Regenerative Medicine, Bioengineering, Swanson School of Engineering, 589 Salk Hall, 3501 Terrace Street, Pittsburgh, PA 15261, Tel. 412 6480108, Fax 412 6246685, ebeniash@pitt.edu; Charles S. Sfeir. DDS, PhD, Associate Professor, Oral Biology, University of Pittsburgh School of Dental Medicine, Center for Craniofacial Regeneration, McGowan Institute for Regenerative Medicine, Bioengineering, Swanson School of Engineering, 552 Salk Hall, 3501 Terrace Street, Pittsburgh, PA 15261, Tel. 412 6481949, Fax 412 6246685, csfeir@pitt.edu.

Intergrin Binding N-linked Glicoproteins) family, which are associated with mineralized tissues (Fisher and Fedarko, 2003), although they were found in other tissues as well (Fisher *et al.*, 2004; Ogbureke and Fisher, 2005).

DMP1 is an acidic protein containing a large number of Ser (22%), Glu (15%) and Asp (13%) amino acids with a calculated pI=4.15 in its nonphosphorylated form (George *et al.*, 1993). In vivo a high proportion of serines in DMP1 are phosphorylated; for example it is estimated that native mouse DMP1 contains 55 phosphates, suggesting that more than half of its serines are phosphorylated (George *et al.*, 1993). In solution, as other SIBLING proteins (Fisher *et al.*, 2001), DMP1 adopts an extended, unstructured conformation (George *et al.*, 1993), while in the presence of calcium it undergoes self-assembly into filaments (He *et al.*, 2005). DMP1 specifically binds to N-telopeptide sequence of collagen and is shown to affect collagen fibrogenesis (He and George, 2004). *In vivo*, secreted DMP1 is cleaved into two fragments, an acidic C-terminal 57 KDa and a 37 KDa N-terminal domain (Qin *et al.*, 2003) which localize differently in the compartments of dentin and the growth plate of bone (Maciejewska *et al.*, 2009). Both *in vitro* and *in vivo* studies suggest that the C-terminal 57 kDaD fragment of DMP1 is primarily responsible for the function of this protein in biomineralization (Maciejewska *et al.*, 2009; Tartaix *et al.*, 2004).

There is a vast body of evidence indicating that DMP1 plays an important role in the biomineralization of dentin and bone. Mutant animals lacking DMP1 gene have severe bone and dentin defects, manifested by widened unmineralized predentin and osteoid and hypomineralized bone and dentin (Ling *et al.*, 2005; Lu *et al.*, 2007). A number of *in vitro* studies indicate that DMP1 strongly influences various aspects of calcium phosphate mineralization. Specifically, the studies of calcium phosphate mineralization in the gelatin gel assays revealed that depending on the phosphorylation level, DMP1 can induce crystal nucleation, inhibit mineralization, and affect crystal size in a concentration dependant manner (Tartaix *et al.*, 2004). Furthermore, DMP1 supramolecular assemblies can control organization of mineral particles *in vitro* and transiently stabilize amorphous calcium phosphate (ACP) (He *et al.*, 2003; He *et al.*, 2005).

Despite numerous studies, the exact role of DMP1 in dentin mineralization is still unclear. Here we present the data from our immunohistochemical studies of fully mineralized rat incisors and the results of *in vitro* mineralization experiments suggesting that DMP1 might play an important role in the mineral formation and organization in the extafibrillar spaces in dentin and specifically in PTD and dentino-enamel boundary (DEB).

Materials and Methods

Immunohistochemistry studies of rat incisors

Two-months-old Wistar rats were euthanized according to an approved protocol. The mandibles were extracted, immediately freeze-dried and mounted in epoxy resin (Epofix, EMS). The erupted portions of mandibular incisors were polished in the transverse plane using a Minimet 1000 polishing machine (Buehler, Lake Buff, IL) using 6, 1 and 0.25 μm Metadi diamond suspensions (Buehler, Lake Buff, IL). To seal the capillaries, i.e. dentinal tubules, the samples were infused with 3% gelatin. The polished samples were covered with 3% gelatin solution at 39°C under vacuum for 1 hour and then let set for an hour at room temperature. The samples were washed in PBS and re-polished with 0.25 μm diamond suspensions to expose the surface of the sample. The samples were etched for 5 min in 2% EDTA and 1% parafolmaldehyde aqueous solution to expose the antigen epitopes, followed by 5 rinses in PBS containing 0.5% BSA (PBS/BSA). The samples were blocked by 2% BSA and 0.15% glycine in PBS for 1 hour at 4°C followed by incubation with donkey Fab2 fragments and rinsed in PBS/BSA 5 times. The samples were incubated with primary rabbit

anti mouse-DMP1 antibodies raised against its C-terminal portion (generous gift by Dr. Chunlin Qin, Baylor College of Dentistry, Dallas, TX) diluted 1:50, 1:100 and 1:1000 in PBS/BSA for 1 hour. The samples were washed in PBS/BSA. The samples were incubated with secondary Alexa-Fluor 488 donkey anti-rabbit antibodies (Molecular Probes) diluted 1:100 in PBS/BSA for 1 hour, followed by 5 rinses in PBS, mounted on dimpled glass slides and storied in a dark container at 4 °C before analysis. Samples were analyzed using Nikon TE2000-e Eclipse light microscope in the epifluorescence mode.

Generation of recombinant DMP1 (rDMP1)

Mouse DMP1 cDNA was inserted into the pGEX vector following its excision from pcDNA3 vector, (a generous gift from Dr. J. Feng (Baylor College of Dentistry, Dallas, TX)). The DMP1-pGEX was then transformed into the bacterial host BL21. Cells were cultured in LB+Amp media overnight at 37°C. Protein expression was induced with 0.4mM IPTG for 2-6 hr. The bacterial lysate was cleared by centrifugation and applied directly to Glutathione Sepharose 4B (Amersham). After washing with PBS, GST-bound protein was eluted with thrombin. Thrombin was removed from eluates with *p*-Aminobenzamidine immobilized on Sepharose 4 Fast Flow matrix (Amersham). The purified protein was electrophoresed on a polyacrylamide gel to verify the molecular mass, and subsequent western blot analysis was carried out.

Generation of recombinant DMP-1 and APMP-1-adenovirus transfection— DMP1 adenovirus was added to MC3T3-E1 cells, which were then grown in serum-free medium for three days. The media were then collected and immediately frozen at -80°C and lyophilized. Samples were resuspended in 6M urea in 20mM Tris-HCl. The cells and ECM were lysed in 4M Guanidine-HCl pH 7.4 in the presence of a protease inhibitor cocktail (C# 118361450011), 1 tablet / 50ml medium and 10mM NaF for several hours. Guanidine buffer was exchanged with 6M Urea in 20mM Tris-HCl using Amicon ultracentrifuge filter units (Millipore C#UFC901024). The samples collected from the media or the cells/matrix were purified by FPLC, using an anion exchange column – HiTrap Q HP ((Cat. no17-1154-01) from GE Healthcare). Proteins were eluted from the column by increasing salt concentration, using an elution buffer containing 6M Urea in 20mM Tris-HCl+ 0.8M NaCl (PH7.2) at a flow rate of 0.4ml/min for 80min. The quality of the protein preparation was assessed using SDS PAGE and western blot, using antibodies generously provided by Dr. J. Feng (Baylor College of Dentistry, Dallas, TX).

Mineralization procedure

Mineralization experiments were performed using a variation of a published “on grid” mineralization technique (Beniash et al., 2005; Deshpande and Beniash, 2008) High purity $CaCl_2 \cdot 2H_2O$, $Na_2HPO_4.7\ H_2O$ were obtained from Sigma-Aldrich. Stock solutions of $CaCl_2$ (6.68mM) $Na_2HPO_4\ 2\ H_2O$ (4mM) were prepared using deionized distilled water (DDW). A 10X PBS buffer with 100 mM sodium phosphate and 1550 mM NaCl was purchased from Fluka. The pH of 10X PBS solution was adjusted to give pH 7.8, when diluted 10 times. DMP1 in urea was dialyzed against DDW and concentrated to 2mg/ml by SpeedVac. The solution was maintained at 4°C for 48h before the experiments.

For mineralization experiments, a 3.4X PBS solution was prepared from 10X PBS stock solution. Equal volumes of aqueous 4mM $Na_2HPO_4 \cdot 2H_2O$, 3.4X PBS, 6.68mM $CaCl_2 \cdot 2H_2O$ and 1mg/ml protein solutions were mixed together to produce mineralization solution containing 9.5mM phosphate, 1.67mM Ca^{2+} and 250μg/mL of the protein, with final pH=7.8. Twenty μL droplets of the solutions were placed in a humidity chamber and carbon-coated TEM grids were placed on top of the droplets. The samples were incubated at 37°C for 16 hours at 100% humidity. After the incubation, the grids were dipped in DDW, blotted

against filter paper and air-dried. Since at the conditions used in the study the mineral is fully mature after 16 hours (Boskey and Posner, 1973; Termine et al., 1970), the effect of rinsing and drying on the samples was mininmal. Some of the samples were demineralized using an aqueous solution containing 2% glutaraldehyde and 1% ethylenediaminetetraacetic acid (EDTA) at pH 8.0 and subsequently stained with 2% Uranyl Acetate in DDW. The samples were rinsed in DDW, air dried and subjected to transmission electron microscopy (TEM) analysis in the bright field mode.

TEM analysis

Transmission electron microscopy (TEM) and selected area electron diffraction (SAED) analysis of the products of the *in vitro* mineralization experiments were carried out using a JEOL 1210 TEM microscope operated at 100 kV and JEOL 2000EX operated at 200 Kv. The micrographs were recorded using an AMT CCD camera (AMT, Danvers, MA). An aluminum film-coated TEM grid (EMS Hatfield, PA) was used as a standard to calibrate SAED patterns for *d*-spacing calculations. The micrographs were analyzed using ImageJ 1.38× image processing software (Bethesda, MD).

Tomography tilt series of mineralized samples were acquired at nominal magnifications of 23,000 to 26,000, using Tecnai 12 transmission electron microscope (FEI, Hillsboro, OR) equipped with a LaB6 filament at 120 KV at the beam density of ~300 e^-/Å. The micrographs were recorded automatically using bottom mounted Gatan 2000 CCD camera (2048×2048 pix, with the physical pixel size of 14 μm. The micrographs were taken in a tilt range from -60° to 60° with of 1° increment from -45° to 45° and 0.5° increment from -60° to -45°and from 45° to 60°. Because of the strong contrast of mineralized samples, the images were aligned using fiducial-less procedure in IMOD reconstruction package (University of Colorado, Boulder, CO) (Kremer et al., 1996). Three-dimensional density maps were reconstructed from the tilt series images using Chimera software (University of California, San Francisco, CA (Goddard et al., 2007)).

Results

Immunohistochemistry of undemineralized rat incisors

In order to reveal the distribution of DMP1 in dentin, we carried out immunohistochemical studies of non-demineralized polished samples of the erupted portions of rat incisors. Demineralization of tooth samples can lead to serious artifacts in the protein distribution, due to the protein removal or dislocation during the demineralization process. This is especially true for areas with high levels of mineralization and low insoluble matrix content, such as PTD. We therefore believe that compared to traditional techniques involving demineralization of the samples, our method allows for more accurate assessment of DMP1 distribution, than traditional techniques involving demineralization of the samples. In the control sample (exposed to secondary antibodies only) no specific fluorescence was observed (Supplementary Figure 1). In the samples exposed to both primary and secondary antibodies, DMP1 signal was stronger in the areas adjacent to the pulp cavity (Figure 1A, B), and gradually decreased toward the dentin-enamel boundary (Figure 1A, D). The analysis of the samples at higher magnification revealed that the DMP1 signal was primarily localized to the peritubular areas (Figure 1C). Our SEM studies of rat dentin suggest that these areas are hypermineralized and lack collagenous fibrillar matrix, which is typical of PTD (Supplementary Figure 2). Interestingly, a strong immunofluorescence signal was detected along the DEB (Figures 1A, D). The band of fluorescence was a couple of microns thick with alternating regions of strong and weak fluorescence (Figure 1D). A faint fluorescence signal was also detected in bulk enamel around the rods (Figure 1D). DMP1 expression has been previously shown in enamel (Maciejewska et al., 2009), hence this

weak fluorescence can reflect the presence of small amounts of DMP1 in enamel, however further experiments are needed to rule out the possibility of this being an artifact.

In vitro mineralization

The mineral phase formed in all experiments was identified as a crystalline apatite, using electron diffraction. Our *in vitro* mineralization experiments revealed that both phosphorylated pDMP1 and nonphosphorylated rDMP1 had a pronounced effect on the size of apatitic crystallites at a concentration of 0.25 mg/ml, in agreement with earlier studies (Tartaix *et al.*, 2004).(Table 1). In both experiments the crystals were significantly smaller than control crystals grown without protein (Supplementary Figure 3, Table 1), and similar in size to bone crystals (Ziv and Weiner, 1994). Remarkably, in the presence of pDMP1 the crystals assembled into large, well organized bundles, which were up to a micron long and 0.25 microns wide. The electron diffraction analysis of the samples revealed that the *c*-axes of the crystals were co-aligned with the axes of the bundles (Figure 2). To gain better understanding of structural organization of the mineral bundles we carried out an electron tomographic reconstruction of one representative bundle. The results of the tomographic reconstruction confirm that the bundles are composed of stacks of plate-shaped mineral particles oriented along the bundle axis (Figure 3; Supplementary movies 1 and 2). Particles with similar structural organization, not associated with collagen fibrils, were previously identified in PTD using electron tomography (Weiner *et al.*, 1999). In contrast, in the control experiments and in the presence of non-phosphorylated rDMP1 the crystals were randomly distributed on the grid with no preferred orientation (Supplementary Figure 3), implying that phosphorylation is essential for the ability of DMP1 to control mineral organization.

We also carried out demineralization of the samples, followed by staining with uranyl acetate to reveal the protein distribution in our samples. The protein was not homogeneously distributed throughout the grid but formed elongated aggregates, similar in size and shape to the mineralized bundles. In some areas filament like structures, aligned with the long axes of the aggregates, were observed (Figure 4) suggesting that the protein could form a self-assembled template for mineral growth.

Discussion

The results of our *in vitro* mineralization studies indicate that phosphorylated DMP1 can induce organization of apatitic crystalites into bundles with their *c*-axes co-aligned with the axis of the bundle. Such crystalline organization is a hallmark of the collagenous mineralized tissues such as bone and dentin, in which crystals in the mineralized collagen fibrils are aligned in the same manner (Weiner and Wagner, 1998). At the same time nonphosphorylated rDMP1 had no effect on the organization of the crystallites in our experiments. These dramatic differences in the effects of prosphorylated and nonphosphorylated DMP1 on the organization of mineral particles *in vivo* suggest that phosphorylation is essential for DMP1 function in biomeralization.

It is believed that formation of the organized mineralized structures in bone and dentin requires both collagen fibrils and acidic macromolecules (Deshpande and Beniash, 2008; George and Veis, 2008). Yet the structures observed in our *in vitro* mineralization experiments formed without collagen fibrils. Although the major type of mineralized structures in the mineralized tissues are mineralized collagen fibrils (Weiner and Wagner, 1998), a sizable portion of the mineral is formed in the extrafibrillar spaces (Bonar et al., 1985; Kinney et al., 2001). Significant amount of mineral was observed on the surface of collagen fibrils and in the extrafibrillar spaces (Bonar et al., 1985; Hassenkam et al., 2004; Landis et al., 1996). Furthermore, it has been shown that the first organized mineral deposits

form outside of the collagen fibrils and the mineralization eventually progresses into the fibrils (Landis *et al.*, 1996). Mineral crystallites in these initial aggregates are not randomly oriented but are organized into parallel arrays which indicates a certain degree of control by matrix macromolecues. The results of our study showing that phosphorylated DMP1 can organize mineral crystallites in the absence of collagen provide support to the notion that it can play a role in the formation of the extrafibrillar protein-mineral structures in bone and dentin.

In crown dentin highly mineralized peritubular areas do not contain collagen fibrils (Gotliv and Veis, 2007; Weiner et al., 1999). Nevertheless, the mineral crystals in PTD are organized into parallel arrays with their *c*-axes co-aligned similarly to mineralized collagen fibrils. These remarkable characteristics of PTD in terms of its protein composition and structural organization led to different scenarios of its formation (Weiner *et al.*, 1999). According to one scenario, PTD initially contains mineralized collagen fibrils. Subsequently, during PTD maturation collagen is removed proteolytically and substituted by mineral, in a way similar to enamel maturation (Weiner *et al.*, 1999). According to another point of view, collagen is never present in PTD and the organization of the mineral is dictated by the resident proteins (Weiner *et al.*, 1999). The mineral bundles formed in the presence of phosphorylated DMP1 obtained in this study closely resemble the crystalline arrays found in PTD (Weiner *et al.*, 1999) in terms of their structural organization and crystal size. This supports the idea that the formation of organized mineral structures in PTD might not require the presence of collagen fibrils at any stage and that noncollagenous acidic proteins, such as phosphorylated DMP1, can control the PTD mineral formation. Furthermore, our immunofluorecsence study, as well as earlier literature reports (Orsini *et al.*, 2008) indicate that DMP1 is primarily concentrated in PTD. A number of studies indicate high phosphorylation levels of the organic matrix in PTD (Gotliv and Veis, 2007; Gotliv and Veis, 2009; Verdelis *et al.*, 2007; Weiner *et al.*, 1999), and although DMP1 and phosphophoryn are the two major phosphoproteins in dentin, phosphophoryn was not observed in PTD. It is therefore quite likely that the major phosphoprotein of PTD is a phosphorylated form of DMP1, which, according to our *in vitro* experiments, is capable of organizing mineral crystals. Furthermore studies of teeth of DMP1 deficient mice reveal that mineralization of PTD mice is severely compromised in these animals, as manifested by widened dentinal tubules, and the absence of characteristic hypermineralized PTD rim around the tubules (Ye *et al.*, 2004). Together, our *in vitro* mineralization experiments and immunofluorescence studies of nondemineralized dentin samples, as well as the literature reports cited above strongly suggest that phosphorylated DMP1 plays a significant role in the control over mineral formation and organization in PTD.

Interestingly, the intensity of DMP1 fluorescence was not homogeneous throughout dentin. It is prominent in proximal dentin surrounding the pulp chamber and fades away toward distal regions of dentin. The reasons for these differences in DMP1 staining are not particularly clear at this point. One possibility is that DMP1 is proteolytically degraded and/or removed from mature PTD. More studies are needed to clarify this puzzle.

Our observation of strong DMP1 signal at the dentino-enamel boundary (DEB) is quite intriguing. It is well established that DMP1 is expressed by ameloblasts prior and during the initial stages of matrix deposition, when the boundary is formed (Dsouza et al., 1997; George et al., 1995; MacDougall et al., 1998). It is therefore likely that it plays an important role in the formation of this interface. There are several types of mineralized structures at the DEB, including mineralized von Korff collagen fibrils and aprismatic enamel containing large needle-like crystals. At the same time, some of the structures found at this interface, such as enamel tufts and spindles are poorly understood. These structures are less mineralized and contain more protein than does the surrounding enamel (Amizuka *et al.*,

1992; Palamara *et al.*, 1989). The mineral crystals associated with these structures are much smaller than enamel crystals and similar to those found in dentin (Amizuka *et al.*, 1992; Palamara *et al.*, 1989), at the same time no collagen has been found in these structures. Our in vitro mineralization experiments and earlier reports (Tartaix *et al.*, 2004) demonstrate that DMP1 controls the size of the crystals. It is therefore feasible that DMP1 can play a role in the formation of aggregates of small crystals at the dentin-enamel boundary similar to those reported in enamel tufts and spindles.

Summary

The results of our in vitro mineralization experiments indicate that DMP1 can regulate crystal size, in agreement with earlier reports (Tartaix *et al.*, 2004). Furthermore, when phosphorylated, DMP1 can organize mineral crystals into parallel arrays with their *c*-axes co-aligned. These data suggest that DMP1 can play a role in organization of extrafibrillar mineral in collagenous mineralized tissues, such as bone and dentin. Our immunofluorecent studies of non-demineralized polished rat incisors show strong DMP1 signal in peritubular dentin and at the dentin-enamel boundary. Based on the fact that peritubular dentin lacks collagen, but contains organized crystalline bundles, similar to those observed in our *in vitro* mineralization experiments with phosphorylated DMP1 we propose the hypothesis that DMP1 plays an essential role in the regulation of mineralization in this area. Furthermore our observation of strong DMP1 signal at the dentin-enamel boundary suggests that it might play a role in the development of this interface and specifically in the formation of tufts and spindles.

Supplementary Material

Refer to Web version on PubMed Central for supplementary material.

Acknowledgments

The study is supported by NIH grants DE016703 to EB and R01 DE016123 to CS. The TEM studies were conducted at the Center for Biologial Imaging, and the Department of Structural Biology, University of Pittsburgh School of Medicine.

References

Almushayt A, Narayanan K, Zaki AE, George A. Dentin matrix protein 1 induces cytodifferentiation of dental pulp stem cells into odontoblasts. Gene Ther. 2006; 13:611–620. [PubMed: 16319946]

Amizuka N, Uchida T, Fukae M, Yamada M, Ozawa H. Ultrastructural and Immunocytochemical Studies of Enamel Tufts in Human Permanent Teeth. Arch Histol Cytol. 1992; 55:179–190. [PubMed: 1497948]

Beniash E, Simmer JP, Margolis HC. The effect of recombinant mouse amelogenins on the formation and organization of hydroxyapatite crystals in vitro. J Struct Biol. 2005; 149:182–190. [PubMed: 15681234]

Bonar LC, Lees S, Mook HA. Neutron diffraction studies of collagen in fully mineralized bone. J Mol Biol. 1985; 181:265–270. [PubMed: 3981637]

Boskey AL, Posner AS. Conversion of amorphous calcium phosphate to microcrystalline hydroxyapatite. A pH-dependent, solution-mediated, solid-solid conversion. The Journal of Physical Chemistry. 1973; 77:2313–2317.

Deshpande AS, Beniash E. Bioinspired Synthesis of Mineralized Collagen Fibrils. Cryst Growth Des. 2008; 8:3084–3090.

Dsouza RN, Cavender A, Sunavala G, Alvarez J, Ohshima T, Kulkarni AB, MacDougall M. Gene expression patterns of murine dentin matrix protein 1 (Dmp1) and dentin sialophosphoprotein

(DSPP) suggest distinct developmental functions in vivo. J Bone Miner Res. 1997; 12:2040–2049. [PubMed: 9421236]

Feng JQ, Ward LM, Liu SG, Lu YB, Xie YX, Yuan BZ, Yu XJ, Rauch F, Davis SI, Zhang SB, Rios H, Drezner MK, Quarles LD, Bonewald LF, White KE. Loss of DMP1 causes rickets and osteomalacia and identifies a role for osteocytes in mineral metabolism. Nat Genet. 2006; 38:1310–1315. [PubMed: 17033621]

Fisher LW, Fedarko NS. Six genes expressed in bones and teeth encode the current members of the SIBLING family of proteins. Connect Tissue Res. 2003; 44:33–40. [PubMed: 12952171]

Fisher LW, Jain A, Tayback M, Fedarko NS. Small integrin binding ligand N-linked glycoprotein gene family expression in different cancers. Clin Cancer Res. 2004; 10:8501–8511. [PubMed: 15623631]

Fisher LW, Torchia DA, Fohr B, Young MF, Fedarko NS. Flexible structures of SIBLING proteins, bone sialoprotein, and osteopontin. Biochem Biophys Res Commun. 2001; 280:460–465. [PubMed: 11162539]

George A, Veis A. Phosphorylated Proteins and Control over Apatite Nucleation, Crystal Growth, and Inhibition. Chem Rev. 2008; 108:4670–4693. [PubMed: 18831570]

George A, Silberstein R, Veis A. In situ hybridization shows dmp1 (AG1) to be a developmentally regulated dentin-specific protein produced by mature odontoblasts. Connect Tissue Res. 1995; 32:389–394.

George A, Sabsay B, Simonian PAL, Veis A. Characterization of a Novel Dentin Matrix Acidic Phosphoprotein - Implications For Induction of Biomineralization. J Biol Chem. 1993; 268:12624–12630. [PubMed: 8509401]

Goddard TD, Huang CC, Ferrin TE. Visualizing density maps with UCSF Chimera. J Struct Biol. 2007; 157:281–287. [PubMed: 16963278]

Gotliv BA, Veis A. Peritubular Dentin, a Vertebrate Apatitic Mineralized Tissue without Collagen: Role of a Phospholipid-Proteolipid Complex. Calcif Tissue Int. 2007; 81:191–205. [PubMed: 17674072]

Gotliv BA, Veis A. The Composition of Bovine Peritubular Dentin: Matching TOF-SIMS, Scanning Electron Microscopy and Biochemical Component Distributions. Cells Tissues Organs. 2009; 189:12–19. [PubMed: 18728348]

Hassenkam T, Fantner GE, Cutroni JA, Weaver JC, Morse DE, Hansma PK. High-resolution AFM imaging of intact and fractured trabecular bone. Bone. 2004; 35:4–10. [PubMed: 15207735]

He G, George A. Dentin matrix protein 1 immobilized on type I collagen fibrils facilitates apatite deposition in vitro. J Biol Chem. 2004; 279:11649–11656. [PubMed: 14699165]

He G, Dahl T, Veis A, George A. Nucleation of apatite crystals in vitro by self-assembled dentin matrix protein, 1. Nat Mater. 2003; 2:552–558. [PubMed: 12872163]

He G, Gajjeraman S, Schultz D, Cookson D, Qin C, Butler WT, Hao J, George A. Spatially and Temporally Controlled Biomineralization Is Facilitated by Interaction between Self-Assembled Dentin Matrix Protein 1 and Calcium Phosphate Nuclei in Solution. Biochemistry (Mosc). 2005; 44:16140–16148.

Hirst KL, IbarakiOconnor K, Young MF, Dixon MJ. Cloning and expression analysis of the bovine dentin matrix acidic phosphoprotein gene. J Dent Res. 1997; 76:754–760. [PubMed: 9109824]

Kinney JH, Pople JA, Driessen CH, Breunig TM, Marshall GW, Marshall SJ. Intrafibrillar Mineral May be Absent in Dentinogenesis Imperfecta Type II (DI-II). J Dent Res. 2001; 80:1555–1559. [PubMed: 11499512]

Kremer JR, Mastronarde DN, McIntosh JR. Computer visualization of three-dimensional image data using IMOD. J Struct Biol. 1996; 116:71–76. [PubMed: 8742726]

Landis WJ, Hodgens KJ, Song MJ, Arena J, Kiyonaga S, Marko M, Owen C, McEwen BF. Mineralization of collagen may occur on fibril surfaces: Evidence from conventional and high-voltage electron microscopy and three-dimensional imaging. J Struct Biol. 1996; 117:24–35. [PubMed: 8776885]

Ling YF, Rios HF, Myers ER, Lu YB, Feng JQ, Boskey AL. DMP1 depletion decreases bone mineralization in vivo: An FTIR imaging analysis. J Bone Miner Res. 2005; 20:2169–2177. [PubMed: 16294270]

Lorenz-Depiereux B, Bastepe M, Benet-Pages A, Amyere M, Wagenstaller J, Muller-Barth U, Badenhoop K, Kaiser SM, Rittmaster RS, Shlossberg AH, Olivares JL, Loris C, Ramos FJ, Glorieux F, Vikkula M, Juppner H, Strom TM. DMP1 mutations in autosomal recessive hypophosphatemia implicate a bone matrix protein in the regulation of phosphate homeostasis. Nat Genet. 2006; 38:1248–1250. [PubMed: 17033625]

Lu YB, Ye L, Yu SB, Zhang SB, Xie YX, McKee MD, Li YC, Kong J, Eick JD, Dallas SL, Feng JQ. Rescue of odontogenesis in Dmp1-deficient mice by targeted re-expression of DMP1 reveals roles for DMP1 in early odontogenesis and dentin apposition in vivo. Dev Biol. 2007; 303:191–201. [PubMed: 17196192]

MacDougall M, Gu TT, Luan XG, Simmons D, Chen JK. Identification of a novel isoform of mouse dentin matrix protein 1: Spatial expression in mineralized tissues. J Bone Miner Res. 1998; 13:422–431. [PubMed: 9525343]

Maciejewska I, Cowan C, Svoboda K, Butler WT, D'Souza R, Qin CL. The NH2-terminal and COOH-terminal Fragments of Dentin Matrix Protein 1 (DMP1) Localize Differently in the Compartments of Dentin and Growth Plate of Bone. J Histochem Cytochem. 2009; 57:155–166. [PubMed: 18854597]

Narayanan K, Srinivas R, Ramachandran A, Hao JJ, Quinn B, George A. Differentiation of embryonic mesenchymal cells to odontoblast-like cells by overexpression of dentin matrix protein 1. Proc Natl Acad Sci U S A. 2001; 98:4516–4521. [PubMed: 11287660]

Ogbureke KUE, Fisher LW. Renal expression of SIBLING proteins and their partner matrix metalloproteinases (MMPs). Kidney Int. 2005; 68:155–166. [PubMed: 15954904]

Orsini G, Ruggeri A, Mazzoni A, Nato F, Falconi M, Putignano A, Di Lenarda R, Nanci A, Breschi L. Immunohistochemical localization of dentin matrix protein 1 in human dentin. Eur J Histochem. 2008; 52:215–220. [PubMed: 19109095]

Palamara J, Phakey PP, Rachinger WA, Orams HJ. The Ultrastructure of Spindles and Tufts in Human Dental Enamel. Adv Dent Res. 1989; 3:249–257. [PubMed: 2640435]

Qin C, Baba O, Butler WT. Post-translational modifications of sibling proteins and their roles in osteogenesis and dentinogenesis. Critical Reviews in Oral Biology & Medicine. 2004; 15:126–136. [PubMed: 15187031]

Qin CL, Brunn JC, Cook RG, Orkiszewski RS, Malone JP, Veis A, Butler WT. Evidence for the proteolytic processing of dentin matrix protein 1 - Identification and characterization of processed fragments and cleavage sites. J Biol Chem. 2003; 278:34700–34708. [PubMed: 12813042]

Tartaix PH, Doulaverakis M, George A, Fisher LW, Butler WT, Qin C, Salih E, Tan M, Fujimoto Y, Spevak L, Boskey AL. In Vitro Effects of Dentin Matrix Protein-1 on Hydroxyapatite Formation Provide Insights into in Vivo Functions. J Biol Chem. 2004; 279:18115–18120. [PubMed: 14769788]

Termine JD, Peckauskas RA, Posner AS. Calcium phosphate formation in vitro : II. Effects of environment on amorphous-crystalline transformation. Arch Biochem Biophys. 1970; 140:318–325. [PubMed: 4319593]

Toyosawa S, Shintani S, Fujiwara T, Ooshima T, Sato A, Ijuhin N, Komori T. Dentin matrix protein 1 is predominantly expressed in chicken and rat osteocytes but not in osteoblasts. J Bone Miner Res. 2001; 16:2017–2026. [PubMed: 11697797]

Verdelis K, Lukashova L, Yamauchi M, Atsawasuwan P, Wright JT, Peterson MGE, Jha D, Boskey AL. Changes in matrix phosphorylation during bovine dentin development. Eur J Oral Sci. 2007; 115:296–302. [PubMed: 17697169]

Weiner S, Wagner HD. The material bone: Structure mechanical function relations. Annual Review of Materials Science. 1998; 28:271–298.

Weiner S, Veis A, Beniash E, Arad T, Dillon JW, Sabsay B, Siddiqui F. Peritubular dentin formation: Crystal organization and the macromolecular constituents in human teeth. J Struct Biol. 1999; 126:27–41. [PubMed: 10329486]

Ye L, MacDougall M, Zhang S, Xie Y, Zhang J, Li Z, Lu Y, Mishina Y, Feng JQ. Deletion of Dentin Matrix Protein-1 Leads to a Partial Failure of Maturation of Predentin into Dentin, Hypomineralization, and Expanded Cavities of Pulp and Root Canal during Postnatal Tooth Development. J Biol Chem. 2004; 279:19141–19148. [PubMed: 14966118]

Ziv V, Weiner S. Bone Crystal Sizes: A Comparison of Transmission Electron Microscopic and X-Ray Diffraction Line Width Broadening Techniques. Connect Tissue Res. 1994; 30:165–175. [PubMed: 8039384]

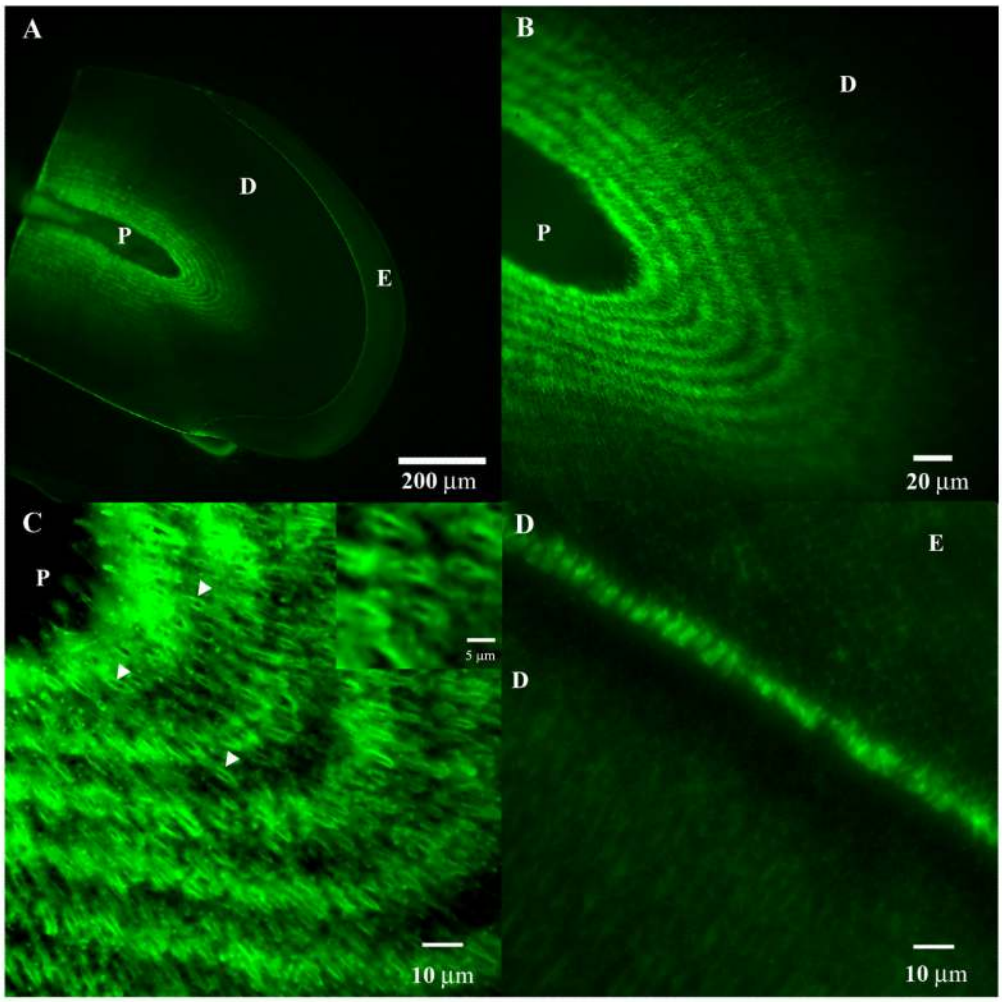

Figure 1.
Epifluorecence micrographs of polished rat incisors stained with antibodies against DMP1. **A.** Low magnification, **B.** Intermediate magnification of an area shown in Figure 1A. **C.** High magnification of an area shown in Figure 1B. Red arrowheads point toward dentinal tubules. Please note that the signal is confined to the peritubular area. **D.** High magnification of the DEB region. D-dentin, E-enamel, P-pulp.

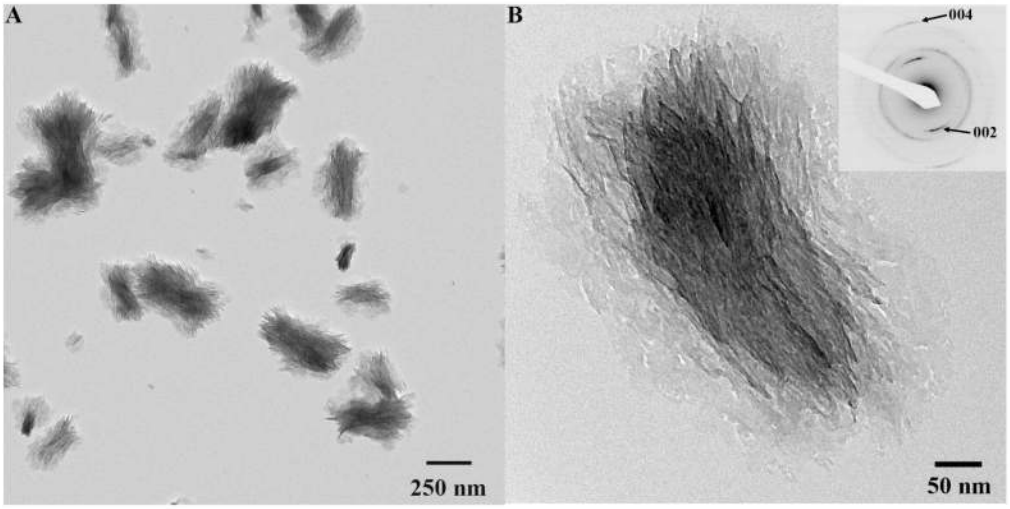

Figure 2.
TEM micrographs of the mineralization reaction products formed in the presence of phosphorylated DMP1. **A.** Low magnification micrograph, showing several mineral bundles. **B.** Micrograph showing an individual crystalline bundle and its diffraction pattern (inset). Note that the *c*-axes of the cryatalitess are preferentially oriented along the bundle axis as indicated by arcs of 002 and 004 reflections.

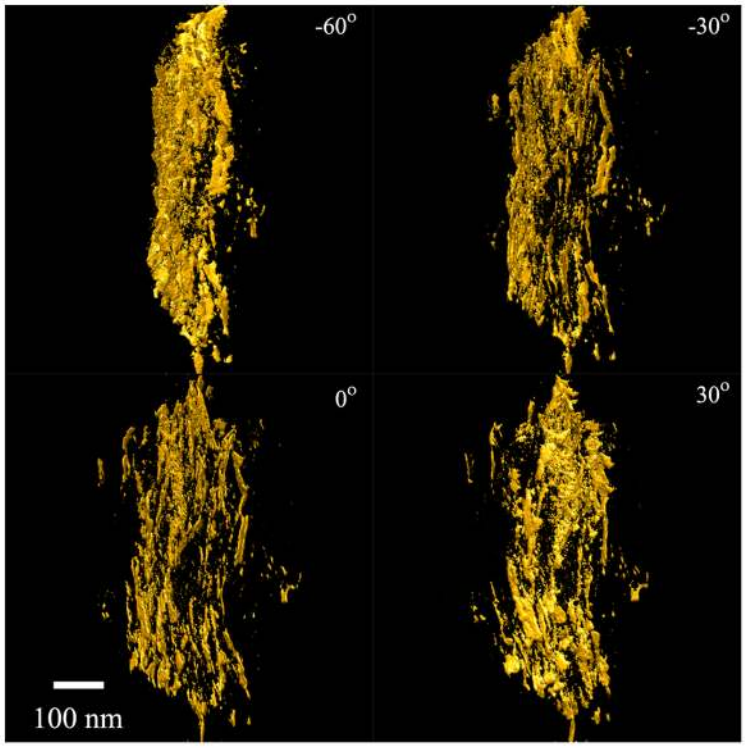

Figure 3.
Tomographic reconstruction of a bundle of crystallites formed in the presence of phosphorylated DMP1 in 4 different orientations.

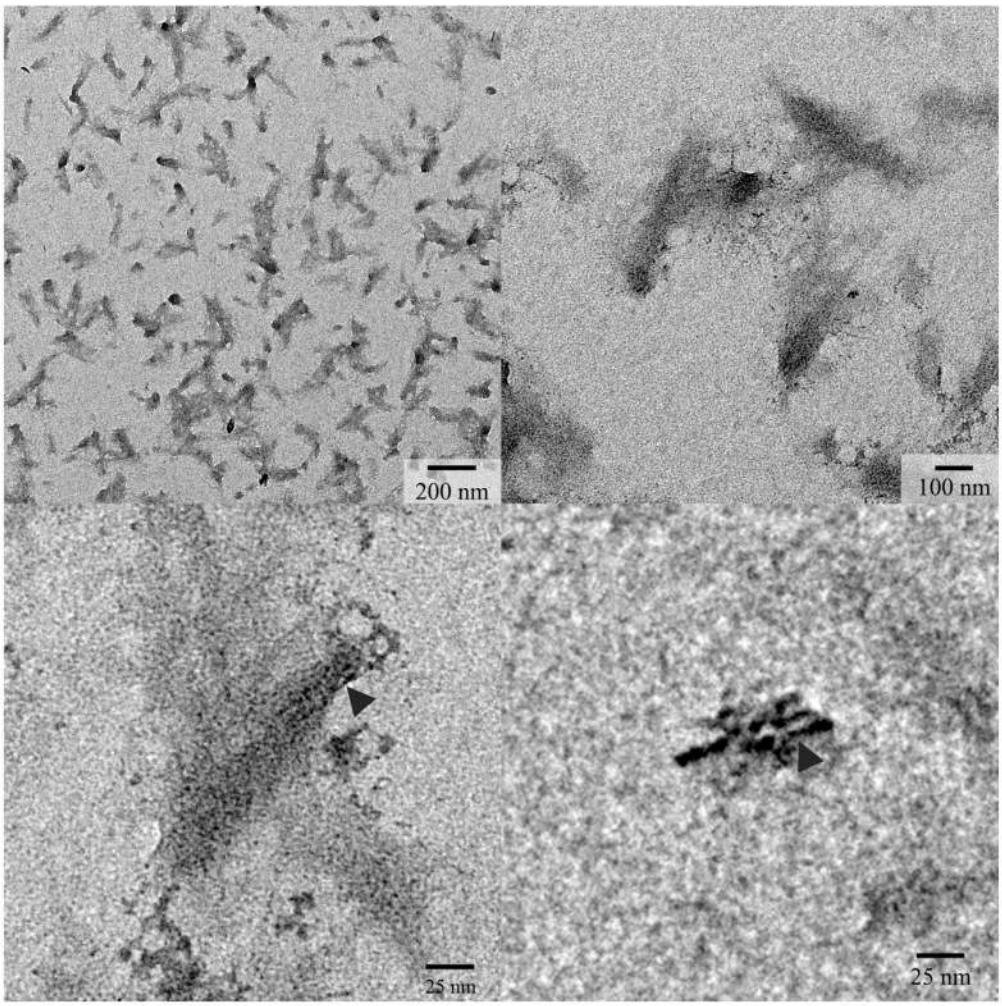

Figure 4.
TEM micrographs of protein aggregates, revealed after demineralization of the mineralization reaction products formed in the presence of phosphorylated DMP1 and stained with uranyl acetate. Note that some of the aggregates contain aligned filament like structures (arrowheads).

Table 1

Sizes of mineral particles formed in the mineralization experiments.

Mineralization experiment	Length (nm)	Width (nm)	Thickness (nm)	Aspect ratio
pDMP1	74.4 ± 24.3*	38.6 ± 8.8	3.05 ± 0.39	1.92
rDMP1	66.03 ± 19.9	34.3 ± 7.4	2.99 ± 0.25	1.94
Control	143.8 ± 53.0	80.0 ± 26.8	3.04 ± 0.34	1.79

*Standard Deviaation